

provided that the energy and orientation requirements for the involved orbitals are respected. We are currently exploring the range 10–11 Å.²¹

Safety Note. Perchlorate salts of metal complexes, with organic ligands are potentially explosive. We used in the synthesis here described only small amounts of material (the preparations were carried out on the millimole scale), and the starting perchlorate

salt was an aquo complex. The dilute solutions were handled with great caution and evaporated slowly at room temperature.

When noncoordinating agents are required, every attempt should be made to substitute anions such as the fluoro sulfonates for the perchlorates.²³

Supplementary Material Available: Listings of atomic parameters for hydrogen atoms (Table VI) and thermal parameters for non-hydrogen atoms (Table VII) (2 pages); a listing of structure factor amplitudes (41 pages). Ordering information is given on any current masthead page.

- (21) Julve, M.; Verdager, M.; Faus, J.; Tinti, F.; Moratal, J.; Monge, A.; Gutierrez-Puebla, E. *Inorg. Chem.*, in press.
 (22) (a) Burns, G. J. *Chem. Phys.* 1964, 41, 1521. (b) Hay, P. J.; Thibeault, J. C.; Hoffmann, R. *J. Am. Chem. Soc.* 1975, 97, 4884.

- (23) Cf.: *J. Chem. Educ.* 1973, 50, A335; 1985, 62, 1001.

Contribution from the Department of Chemistry, Memorial University of Newfoundland, St. John's, Newfoundland, Canada A1B 3X7, and Chemistry Division, National Research Council, Ottawa, Ontario, Canada K1A 0R6

Spontaneous Reduction of Copper(II) Complexes of the Ligand 3,6-Bis(2-pyridylthio)pyridazine. Crystal Structures of Bis[3,6-bis(2-pyridylthio)pyridazine-*N*¹,*N*²]aqua copper(II) Diperchlorate Trihydrate and Bis[μ-3,6-bis(2-pyridylthio)pyridazine-*N*⁴, μ-*N*¹, μ-*N*², *N*³]dicopper(I) Diperchlorate

Sanat K. Mandal,^{1a} Laurence K. Thompson,^{*1a} Eric J. Gabe,^{†1b} Florence L. Lee,^{1b} and Jean-Pierre Charland^{1b}

Received December 16, 1986

The ligand 3,6-bis(2-pyridylthio)pyridazine (PTP) forms both mononuclear and binuclear copper(II) derivatives and binuclear copper(I) derivatives. The copper(II) complexes reported are characterized by exhibiting positive reduction potentials (+0.4 to +0.6 V vs. SCE), a feature that can be exploited with respect to the redox chemistry of such systems. The complexes [Cu(PTP)₂(H₂O)](ClO₄)₂·3.3H₂O (I) and [Cu₂(PTP)Cl₄]·CH₃CH₂OH (III) both react with appropriate reducing agents (e.g. I⁻, SO₃²⁻) to produce derivatives containing the very stable species [Cu₂(PTP)₂]²⁺, involving two four-coordinate copper(I) centers. The crystal and molecular structures of [Cu(PTP)₂(H₂O)](ClO₄)₂·3.3H₂O (I) and [Cu₂(PTP)₂](ClO₄)₂ (II) are reported. I crystallizes in the monoclinic system, space group *C*2/*c*, with *a* = 25.176 (7) Å, *b* = 12.6423 (14) Å, *c* = 13.908 (4) Å, β = 122.630 (19)°, and four formula units per unit cell. II crystallizes in the monoclinic system, space group *P*2₁/*a*, with *a* = 8.906 (4) Å, *b* = 18.825 (3) Å, *c* = 10.157 (2) Å, β = 99.82 (0)°, and four formula units per unit cell. Compound III exhibits moderate antiferromagnetic exchange with *g* = 2.03 and -2*J* = 131 cm⁻¹.

Introduction

The spontaneity of the reduction of copper(II) species to copper(I) is influenced to a large extent by the ligand environment at the copper center and by the metal ion stereochemistry. π-Acid ligands generate a more favorable thermodynamic situation for reduction than non-π-acid ligands, and some sulfur donors and acetonitrile generate positive enough reduction potentials that in many cases relatively stable copper(I) species can be generated.^{2,3} Typically, copper(I) salts are generated in acetonitrile (e.g. [Cu(CH₃CN)₄]X; X = ClO₄, BF₄, etc.). Markedly positive Cu(II)/Cu(I) redox potentials (+0.10 to +0.80 V vs. SHE) are found for the type 1 copper protein centers, which contain imidazole (histidine), thioether (methionine), and thiolate (cysteine) donor groups.⁴ Also, positive reduction potentials are found for binuclear copper proteins (fungal laccase, *E*_{1/2} +0.78 V;⁵ tree laccase, *E*_{1/2} +0.43 V;⁵ tyrosinase, *E*_{1/2} +0.30 V;⁶ potentials vs. SHE²). We have examined a number of hydroxide-bridged binuclear copper(II) complexes of tetradentate (N₄) ligands derived from pyridazine and phthalazine, and almost without exception, these systems exhibit positive redox potentials (+0.2 to +0.8 V vs. SCE), spanning the range observed for the binuclear copper proteins.⁷⁻¹¹

In this report we describe some aspects of the copper coordination chemistry of the ligand PTP (3,6-bis(2-pyridylthio)pyridazine; Figure 1) and in particular the spontaneous redox reactions of both mononuclear and binuclear copper(II) complexes of PTP, which exhibit very positive redox potentials. The

square-pyramidal, mononuclear complex [Cu(PTP)₂(H₂O)](ClO₄)₂·3.3H₂O (I), which has been characterized by X-ray crystallography, has a redox potential of +0.57 V (glassy carbon, CH₃CN, TEAP (tetraethylammonium perchlorate), vs. SCE)⁸ and is spontaneously reduced on refluxing in methanol or acetonitrile, for an extended period of time, to [Cu₂(PTP)₂](ClO₄)₂ (II). This binuclear copper(I) species can be generated directly from PTP and cuprous perchlorate (CH₃CN), and an X-ray structure reveals a dimeric, binuclear structural arrangement involving two pseudotetrahedral copper(I) centers. The same product arises on reaction of I with triphenylphosphine in acetonitrile. The complex [Cu₂(PTP)Cl₄]·CH₃CH₂OH (III), the

- (1) (a) Memorial University of Newfoundland. (b) National Research Council.
 (2) Phillips, C. S. G.; Williams, R. J. P. *Inorganic Chemistry*; Oxford University Press: London, 1966; Vol. II, p 316.
 (3) Patterson, G. S.; Holm, R. H. *Bioinorg. Chem.* 1975, 4, 257.
 (4) Addison, A. W. In *Copper Coordination Chemistry: Biochemical and Inorganic Perspectives*; Karlin, K. D., Zubieta, J., Eds.; Adenine: Guilderland, NY, 1984; p 109.
 (5) Reinhammar, B. R. M. *Biochim. Biophys. Acta* 1972, 275, 245.
 (6) Makino, N.; McMahl, P.; Mason, H. S. *J. Biol. Chem.* 1974, 249, 6062.
 (7) Mandal, S. K.; Thompson, L. K.; Hanson, A. W. *J. Chem. Soc., Chem. Commun.* 1985, 1709.
 (8) Woon, T. C.; McDonald, R.; Mandal, S. K.; Thompson, L. K.; Addison, A. W. *J. Chem. Soc., Dalton Trans.* 1986, 2381.
 (9) Mandal, S. K.; Woon, T. C.; Thompson, L. K.; Newlands, M. J.; Gabe, E. J. *Aust. J. Chem.* 1986, 39, 1007.
 (10) Thompson, L. K.; Mandal, S. K.; Gabe, E. J.; Lee, F. L.; Addison, A. W. *Inorg. Chem.* 1987, 26, 657.
 (11) Mandal, S. K.; Thompson, L. K.; Newlands, M. J.; Lee, F. L.; LePage, Y.; Charland, J.-P.; Gabe, E. J. *Inorg. Chim. Acta* 1986, 122, 199.

* To whom correspondence should be addressed.

† This paper assigned NRCC Contribution No. 27819.

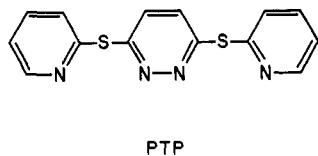


Figure 1. Structure of PTP.

structure of which has already been reported¹¹ ($E_{1/2} = +0.48$ V; Pt, CH₃CN, TEAP, vs. SCE), reacts rapidly with aqueous iodide to give [Cu₂(PTP)₂](I₃)₂, which on recrystallization from acetonitrile gives IV, a binuclear copper(I) species with a cation identical with that of II. The same species also results when I reacts with iodide in aqueous acetonitrile.

Experimental Section

Electrochemical Measurements. The electrochemical experiments were performed at room temperature in dimethylformamide (spectroscopic grade, dried over molecular sieves) and acetonitrile (spectroscopic grade, dried over molecular sieves) under O₂-free conditions with a BAS CV27 voltammograph and a Houston Omnigraph 2000 XY recorder. A three-electrode system was used (cyclic voltammetry) in which the working electrode was either glassy carbon or platinum and the counter electrode platinum, with a standard calomel (SCE) electrode as reference. For coulometry measurements a three-electrode system was employed consisting of a platinum-mesh-flag working electrode, a platinum-mesh counter electrode, and a SCE reference electrode. The supporting electrolyte was tetraethylammonium perchlorate (TEAP, 0.1 M), and all solutions were 10⁻³–10⁻⁴ M in the complex. The best combination of experimental conditions (working electrode, scan rates, solvent, etc.) was determined by preliminary experiment. Reported potentials are uncorrected for junction potentials, and peak separations are not corrected for *iR* drop.

Magnetic Measurements. Room-temperature magnetic moments were measured by the Faraday method with a Cahn 7600 Faraday magnetic susceptibility system. Variable-temperature magnetic susceptibility data were obtained in the range 5–300 K (compound III) with an Oxford Instruments superconducting Faraday magnetic susceptibility system and a Sartorius 4432 microbalance. A main solenoid field of 1.5 T and a gradient field of 10 T m⁻¹ were employed.

Synthesis of PTP and Its Copper Complexes. The syntheses of PTP⁸ and the complexes [Cu(PTP)₂(H₂O)](ClO₄)₂·3.3H₂O (I)⁸ and [Cu₂(PTP)Cl₄·CH₃CH₂OH (III) have already been reported.¹¹ The sample of compound I used in this study gave the following elemental analysis. Anal. Calcd for [Cu(C₁₄H₁₀N₄S₂)₂](H₂O)](ClO₄)₂·3.3H₂O: C, 35.90; H, 3.06; N, 11.97. Found: C, 35.93; H, 2.84; N, 11.80.

[Cu₂(PTP)₂](ClO₄)₂ (II). PTP (1.49 g; 5.00 mmol) was dissolved in boiling acetonitrile (75 mL) under a nitrogen atmosphere and an acetonitrile solution (30 mL) of [Cu(CH₃CN)₄](ClO₄) (1.64 g; 5.00 mmol) added. The resulting mixture was allowed to stand at room temperature in an open beaker. After several days of evaporation red crystals formed, which were filtered off, washed with chloroform, and dried under vacuum (yield 2.30 g). This complex is stable on exposure to air. Anal. Calcd for [Cu₂(C₁₄H₁₀N₄S₂)₂](ClO₄)₂: C, 36.44; H, 2.17; N, 12.15. Found: C, 36.37; H, 2.23; N, 12.12.

[Cu₂(PTP)₂](I₃)₂(CH₃CN)₂ (IV). [Cu₂(PTP)Cl₄·CH₃CH₂OH (1.18 g; 2.00 mmol) was dissolved in water (40 mL), and an aqueous solution (10 mL) of sodium iodide (0.90 g; 4.0 mmol) was added slowly with stirring. A brown precipitate formed, which was separated by filtration, washed several times with water and ethanol, and then extracted with boiling acetonitrile. Slow evaporation of the acetonitrile solution gave dark brown crystals, which were filtered off, washed with chloroform and ethanol, and dried under vacuum (yield 0.67 g). Anal. Calcd for [Cu₂(C₁₄H₁₀N₄S₂)₂](I₃)(C₂H₅N)₂: C, 24.50; H, 1.66; N, 8.93; I, 48.63. Found: C, 24.27; H, 1.64; N, 8.77; I, 50.34.

Crystallographic Data Collection and Refinement of the Structures. [Cu(PTP)₂(H₂O)](ClO₄)₂·3.3H₂O (I). Crystals of I are deep blue. The diffraction intensities of an approximately 0.3 × 0.2 × 0.1 mm crystal were collected with graphite-monochromatized Mo K α radiation by using the $\theta/2\theta$ scan technique with profile analysis¹² to $2\theta_{\max} = 50^\circ$ on a Picker four-circle diffractometer. A total of 3482 reflections were measured, of which 3294 were unique and 1343 reflections were considered significant with $I_{\text{net}} > 2.5\sigma(I_{\text{net}})$. Lorentz and polarization factors were applied, but no correction was made for absorption. The cell parameters were obtained by the least-squares refinement of the setting angles of 34 reflections with $2\theta > 35^\circ$ ($\lambda(\text{Mo K}\alpha_1) = 0.70930 \text{ \AA}$).

Table I. Crystal Data

	Cu ₂ C ₂₈ H ₂₂ Cl ₂ N ₈ O ₉ S ₄ ·3.3H ₂ O (I)	Cu ₂ C ₂₈ H ₂₀ Cl ₂ N ₈ O ₈ S ₄ (II)
cryst syst	monoclinic	monoclinic
space group	C2/c	P2 ₁ /a
a, Å	25.176 (7)	8.906 (4)
b, Å	12.6423 (14)	18.825 (3)
c, Å	13.908 (4)	10.157 (2)
β , deg	122.630 (19)	99.82 (0)
V, Å ³	3728.15	1677.93
Z	4	4
ρ (calcd), g cm ⁻³	1.67	1.86
μ , mm ⁻¹	1.01	5.90
radiation; λ , Å	Mo K α_1 ; 0.70930	Cu K α ; 1.54178
temp for data	296	120
collecn, K		
min and max transmission	0.89, 0.91	
octants of data collcd	<i>h</i> , 29 → 29; <i>k</i> , 0 → 15; <i>l</i> , 0 → 16	<i>h</i> , -11 → 11; <i>k</i> , 0 → 22; <i>l</i> , 0 → 12
GOF	1.88	10.05

Table II. Final Atomic Positional Parameters and Equivalent Isotropic Debye-Waller Temperature Factors (Esd's) for [Cu(PTP)₂(H₂O)](ClO₄)₂·3.3H₂O

atom	<i>x</i>	<i>y</i>	<i>z</i>	<i>B</i> _{iso} , Å ³
Cu	1 (0)	0.19545 (16)	0 (0)	2.67 (14)
Cl	0.14086 (17)	0.9950 (3)	0.8063 (3)	5.30 (26)
S(1)	0.54134 (15)	0.3856 (3)	0.4225 (3)	4.46 (26)
S(2)	0.32575 (16)	0.1051 (3)	0.3630 (3)	5.22 (27)
O(11)	0.1908 (4)	0.9558 (9)	0.8039 (10)	11.2 (10)
O(12)	0.1412 (5)	0.9591 (9)	0.9029 (9)	10.4 (10)
O (13)	0.1433 (4)	1.1056 (8)	0.8108 (8)	7.8 (8)
O(14)	0.0840 (4)	0.9619 (8)	0.7092 (8)	8.6 (7)
O(1)	0.5000 (0)	0.0265 (9)	0.2500 (0)	5.5 (9)
O(2)	0.0000 (0)	0.1669 (11)	0.2500 (0)	9.7 (13)
O(3)	0.5146 (8)	0.0205 (15)	0.9551 (14)	7.3 (15)
N(1)	0.5864 (4)	0.2055 (8)	0.3942 (7)	3.0 (6)
N(2)	0.4622 (4)	0.2443 (7)	0.3417 (7)	2.5 (6)
N(3)	0.4164 (4)	0.1623 (8)	0.3289 (7)	3.1 (6)
N(4)	0.3845 (5)	-0.0673 (10)	0.3459 (9)	5.5 (8)
C(1)	0.6312 (6)	0.1325 (9)	0.4196 (9)	3.6 (8)
C(2)	0.6915 (9)	0.1445 (11)	0.5133 (11)	4.8 (9)
C(3)	0.7051 (6)	0.2300 (13)	0.5819 (11)	5.4 (10)
C(4)	0.6597 (6)	0.3009 (12)	0.5602 (11)	4.8 (9)
C(5)	0.5994 (5)	0.2885 (10)	0.4615 (10)	3.7 (8)
C(6)	0.4803 (5)	0.3044 (10)	0.4121 (10)	3.1 (8)
C(7)	0.4536 (6)	0.3331 (9)	0.4722 (10)	3.9 (10)
C(8)	0.4057 (6)	0.2702 (11)	0.4576 (11)	4.1 (10)
C(9)	0.3888 (5)	0.1837 (11)	0.3838 (10)	3.6 (9)
C(10)	0.3313 (6)	-0.0074 (11)	0.2909 (12)	5.1 (10)
C(11)	0.2805 (6)	-0.0371 (13)	0.1816 (14)	6.7 (12)
C(12)	0.2856 (8)	-0.1270 (13)	0.1330 (13)	7.3 (13)
C(13)	0.3384 (8)	-0.1864 (13)	0.1883 (14)	7.1 (12)
C(14)	0.3861 (7)	-0.1545 (12)	0.2908 (14)	6.4 (13)
O(4)	0.5190 (13)	-0.0564 (22)	0.3268 (24)	21.7 (14)
H(1)	0.620 (0)	0.062 (0)	0.365 (0)	4.3 (0)
H(2)	0.730 (0)	0.087 (0)	0.534 (0)	5.1 (0)
H(3)	0.753 (0)	0.242 (0)	0.657 (0)	5.5 (0)
H(4)	0.669 (0)	0.371 (0)	0.618 (0)	5.3 (0)
H(7)	0.470 (0)	0.402 (0)	0.531 (0)	5.1 (0)
H(8)	0.380 (0)	0.287 (0)	0.500 (0)	5.2 (0)
H(11)	0.237 (0)	0.014 (0)	0.137 (0)	6.1 (0)
H(12)	0.244 (0)	-0.150 (0)	0.047 (0)	6.9 (0)
H(13)	0.341 (0)	-0.259 (0)	0.145 (0)	6.8 (0)
H(14)	0.429 (0)	-0.202 (0)	0.337 (0)	7.0 (0)

The structure was solved by direct methods using MULTAN¹³ and refined by full-matrix least-squares methods to final residuals of $R_f = 0.057$ and $R_w = 0.032$ for the significant data (0.170 and 0.038 for all data) with weights based on counting statistics. H atom positions were calculated but not refined. O(3)(H₂O) and O(4)(H₂O) were refined with occupancies of 0.5505 and 0.5995, respectively, leading to 3.3 lattice water molecules, in agreement with C, H, N analytical data. Crystal

(12) Grant, D. F.; Gabe, E. J. *J. Appl. Crystallogr.* 1978, 11, 114.(13) Germain, G.; Main, P.; Woolfson, M. M. *Acta Crystallogr., Sect. A: Cryst. Phys., Diffr., Theor. Gen. Crystallogr.* 1971, A27, 368.

Table III. Final Atomic Positional Parameters and Equivalent Isotropic Debye–Waller Temperature Factors (E_{sd}) for $[\text{Cu}_2(\text{PTP})_2](\text{ClO}_4)_2$ (II)

atom	x	y	z	$B_{\text{iso}}, \text{\AA}^2$
Cu	1.06684 (6)	0.940465 (25)	-0.10345 (5)	1.10 (2)
Cl	0.66896 (10)	1.13484 (4)	-0.37213 (8)	1.38 (4)
S(1)	0.80462 (11)	0.99645 (4)	0.34766 (8)	1.25 (4)
S(2)	1.05763 (11)	0.78021 (4)	-0.02350 (8)	1.34 (4)
O(1)	0.7558 (3)	1.19990 (13)	-0.34676 (25)	1.85 (11)
O(2)	0.7580 (3)	1.07581 (13)	-0.31025 (27)	2.18 (11)
O(3)	0.6310 (3)	1.12272 (15)	-0.51282 (25)	2.42 (12)
O(4)	0.5304 (3)	1.14097 (13)	-0.31543 (25)	1.81 (11)
N(1)	0.9988 (3)	0.90869 (14)	0.0656 (3)	0.90 (12)
N(2)	0.9447 (3)	0.95536 (14)	0.1478 (3)	0.93 (12)
N(3)	0.7094 (3)	1.06623 (14)	0.1166 (3)	1.03 (12)
N(4)	0.9356 (3)	0.86948 (14)	-0.2199 (3)	1.09 (13)
C(1)	0.8783 (4)	0.93186 (17)	0.2483 (3)	1.00 (14)
C(2)	0.8676 (4)	0.85899 (18)	0.2764 (3)	1.32 (15)
C(3)	0.9253 (4)	0.81182 (19)	0.1949 (3)	1.25 (15)
C(4)	0.9858 (4)	0.83870 (17)	0.0887 (3)	0.90 (14)
C(5)	0.6626 (4)	1.03481 (17)	0.2210 (3)	1.08 (15)
C(6)	0.5107 (5)	1.03034 (20)	0.2341 (4)	1.41 (15)
C(7)	0.4026 (5)	1.05844 (20)	0.1339 (4)	1.77 (17)
C(8)	0.4496 (5)	1.09066 (16)	0.0257 (4)	1.59 (16)
C(9)	0.6029 (5)	1.09339 (18)	0.0204 (4)	1.22 (16)
C(10)	0.9324 (4)	0.80235 (18)	-0.1762 (3)	1.18 (15)
C(11)	0.8382 (5)	0.75024 (21)	-0.2426 (3)	1.76 (17)
C(12)	0.7415 (5)	0.76839 (22)	-0.3582 (4)	1.94 (17)
C(13)	0.7394 (5)	0.83785 (22)	-0.4031 (4)	1.73 (17)
C(14)	0.8384 (4)	0.88613 (21)	-0.3331 (3)	1.38 (15)
H(2)	0.820 (4)	0.8451 (17)	0.355 (3)	0.6 (7)
H(3)	0.924 (4)	0.7639 (18)	0.207 (3)	0.8 (7)
H(6)	0.487 (4)	1.0117 (19)	0.302 (4)	1.6 (9)
H(7)	0.298 (5)	1.0547 (19)	0.135 (4)	1.6 (8)
H(8)	0.381 (4)	1.1095 (20)	-0.049 (4)	1.8 (8)
H(9)	0.633 (4)	1.1105 (18)	-0.048 (3)	0.6 (7)
H(11)	0.842 (4)	0.7081 (20)	-0.206 (4)	1.5 (8)
H(12)	0.685 (4)	0.7343 (19)	-0.404 (3)	1.2 (8)
H(13)	0.674 (5)	0.8519 (20)	-0.479 (4)	2.2 (9)
H(14)	0.847 (4)	0.9312 (20)	-0.360 (4)	1.9 (9)

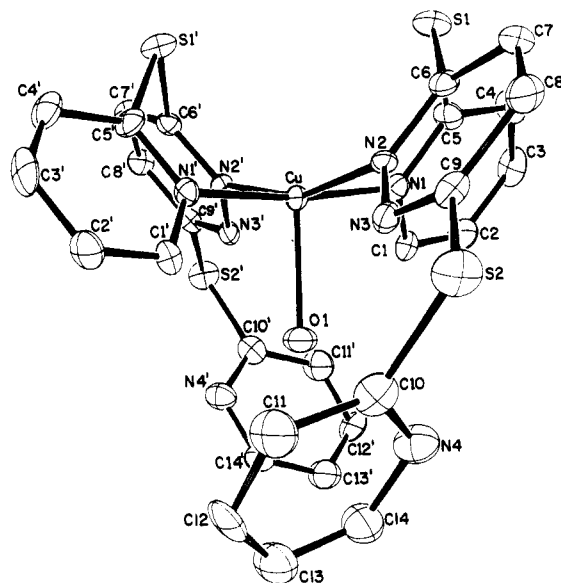
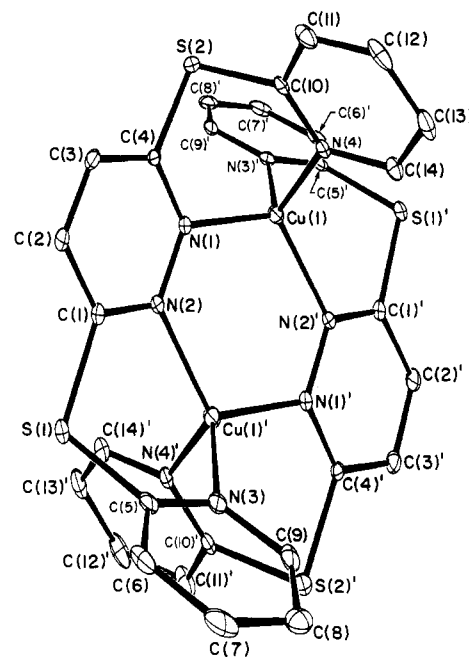
data are given in Table I, and final atomic positional parameters and equivalent isotropic temperature factors are listed in Table II. All calculations were performed with the NRCVAX system of programs,¹⁴ and scattering factors were taken from ref 15. Anisotropic thermal parameters (Table SI) and a listing of structure factors (Table SII) are included as supplementary material.

$[\text{Cu}_2(\text{PTP})_2](\text{ClO}_4)_2$ (II). Crystals of II are red. The diffraction intensities of an approximately $0.35 \times 0.25 \times 0.1$ mm rectangular platelet were collected with graphite-monochromatized Cu $K\alpha$ radiation by using the $\theta/2\theta$ scan technique with profile analysis¹² to $2\theta_{\text{max}} = 118^\circ$ on a Picker four-circle diffractometer at 120 K. A total of 2996 reflections were measured, of which 2447 were unique and 2384 were considered significant with $I_{\text{net}} > 2.5\sigma(I_{\text{net}})$. Lorentz and polarization factors were applied, but no correction was made for absorption. The cell parameters were obtained by the least-squares refinement of the setting angles of 46 reflections with $2\theta = 113\text{--}119^\circ$ ($\lambda(\text{Cu } K\alpha) = 1.54178 \text{ \AA}$).

The structure was solved by direct methods using MULTAN¹³ and refined by full-matrix least-squares methods to final residuals of $R_f = 0.035$ and $R_w = 0.039$ for the significant data (0.036 and 0.039 for all data) with weights based on counting statistics. Crystal data are given in Table I, and final atomic positional parameters and equivalent isotropic temperature factors are listed in Table III. All calculations were performed with the NRCVAX system of programs,¹⁴ and scattering factors were taken from ref 15. Anisotropic thermal parameters (Table SIII) and a listing of structure factors (Table SIV) are included as supplementary material.

Results and Discussion

Description of the Structures of $[\text{Cu}(\text{PTP})_2(\text{H}_2\text{O})](\text{ClO}_4)_2 \cdot 3.3\text{H}_2\text{O}$ (I) and $[\text{Cu}_2(\text{PTP})_2](\text{ClO}_4)_2$ (II). The structure of I is shown in Figure 2, and interatomic distances and angles relevant to the copper coordination sphere are given in Table IV. A

**Figure 2.** Structural representation of $[\text{Cu}(\text{PTP})_2(\text{H}_2\text{O})]^{2+}$ with hydrogen atoms omitted (40% probability thermal ellipsoids).**Figure 3.** Structural representation of $[\text{Cu}_2(\text{PTP})_2]^{2+}$ with hydrogen atoms omitted (40% probability thermal ellipsoids).**Table IV.** Interatomic Distances (\AA) and Angles (deg) Relevant to the Copper Coordination Sphere in $[\text{Cu}(\text{PTP})_2(\text{H}_2\text{O})](\text{ClO}_4)_2 \cdot 3.3\text{H}_2\text{O}$ (I)

Cu–O(1)	2.136 (11)	Cu–N(2)	1.993 (9)
Cu–N(1)	2.016 (8)		
O(1)–Cu–N(1)	93.6 (3)	N(2)–Cu–N(2)	158.9 (4)
O(1)–Cu–N(2)	100.5 (3)	N(1)–Cu–N(2)	89.0 (4)
N(1)–Cu–N(1)	172.8 (4)	N(1)–Cu–N(2)	89.7 (4)

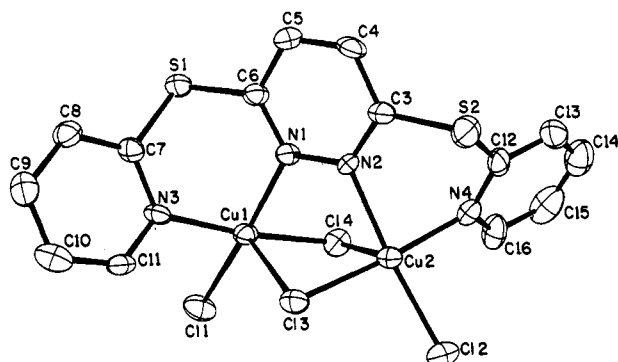
preliminary report of the structure of this compound appears elsewhere.⁸ The mononuclear cation $[\text{Cu}(\text{PTP})_2(\text{H}_2\text{O})]^{2+}$ consists of a distorted square-pyramidal copper(II) center with relatively short in-plane copper–nitrogen distances involving just two nitrogen donors of each ligand and a short axial interaction to a water molecule ($\text{Cu–O}(1) = 2.14(1) \text{ \AA}$). One pyridine nitrogen ($\text{N}(1)$) and one pyridazine nitrogen ($\text{N}(2)$) generate a six-membered chelate ring with a well-formed boat conformation having an angle of $99.2(5)^\circ$ at the exocyclic sulfur atom ($\text{S}(1)$). The major equatorial distortion involves the $\text{N}(2)\text{–Cu–N}(2)$ angle of $158.9(4)^\circ$. The water molecule ($\text{O}(1)$) is enclosed in a cavity created

(14) Gabe, E. J.; Lee, F. L.; LePage, Y. In *Crystallographic Computing III*; Sheldrick, G.; Kruger, C.; Goddard, R., Eds.; Clarendon: Oxford, England, 1985; p 167.

(15) *International Tables for X-ray Crystallography*; Kynoch: Birmingham, England, 1974; Vol. IV, Table 2.2B, p 99.

Table V. Interatomic Distances (Å) and Angles (deg) Relevant to the Copper Coordination Spheres in $[\text{Cu}_2(\text{PTP})_2](\text{ClO}_4)_2$ (II)

Cu(1)–N(1)	2.008 (3)	Cu(1)–N(3)'	2.024 (3)
Cu(1)–N(2)'	2.011 (3)	Cu(1)–N(4)	2.020 (3)
N(1)–Cu(1)–N(2)'	118.1 (1)	N(3)'–Cu(1)–N(4)	113.5 (1)
N(2)'–Cu(1)–N(3)'	93.4 (1)	N(1)–Cu(1)–N(4)	94.30 (1)
N(3)'–Cu(1)–N(1)	118.8 (1)	N(2)'–Cu(1)–N(4)	120.8 (1)

**Figure 4.** Structural representation of $[\text{Cu}_2(\text{PTP})\text{Cl}_4]\cdot\text{CH}_3\text{CH}_2\text{OH}$ (III) with hydrogen atoms and ethanol omitted (40% probability thermal ellipsoids).

by the dangling, noncoordinating, pyridine groups of the two ligands. A distance of 3.76 Å exists between O(1) and the mean plane of the pyridine rings, with a distance of 3.54 Å separating O(1) and N(4). The formation of mononuclear copper derivatives with potentially binucleating tetradentate (N_4) ligands of this sort has been observed before and usually results when the anionic group in question is a poor donor and cannot complete the copper coordination spheres in a potentially binuclear derivative.^{8,16,17}

The structure of II is shown in Figure 3, and interatomic distances and angles relevant to the copper coordination spheres are given in Table V. The binuclear cation consists of two pseudotetrahedral copper(I) centers, separated by 3.422 (1) Å and bridged by two pyridazine groups with terminal pyridine donors completing the four-coordination. The copper–nitrogen separations (2.008–2.024 Å) are relatively short and compare very closely with those obtained for similar bonds in I and in other tetrahedral copper(I) complexes with nitrogen donor ligands.^{18,19} A similar binuclear copper(I) structure has been reported recently in which the two copper atoms are found within a tetradentate macrocyclic N_4 ligand and bridged by two pyridazine moieties.²⁰ However, in this case a much shorter Cu–Cu separation (3.15 Å) exists, resulting, no doubt, from the fact that the bridging pyridazine ligands are only bidentate in nature.

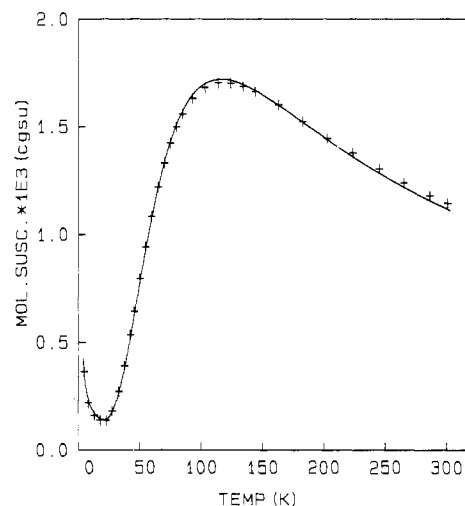
An X-ray structural investigation of IV has shown that it contains the same binuclear copper(I) cation as found in II with triiodide ion and acetonitrile in the lattice. The results of this determination will be reported elsewhere.²¹

Spectral, Magnetic, Electrochemical, and Redox Properties. The spectral, magnetic, and electrochemical properties of I have been reported previously.⁸ The bidentate coordination of the ligand PTP in this complex is unusual but can be assigned on the basis of two bands in the infrared region associated with pyridine ring vibrations. A band at 1026 cm^{-1} is assigned to coordinated pyridine, while an absorption at 1000 cm^{-1} is assigned to unco-

Table VI. Magnetic and Electrochemical Data

compd	color	μ_{eff} (room temp), μ_B	$E_{1/2}$, V vs. SCE	ΔE_p , mV ^a
$[\text{Cu}(\text{PTP})_2(\text{H}_2\text{O})](\text{ClO}_4)_2\cdot 3.3\text{H}_2\text{O}$ (I)	blue	1.86	0.57 ^b	200
$[\text{Cu}_2(\text{PTP})_2](\text{ClO}_4)_2$ (II)	red	diamag	0.19 ^c	200
			0.56 ^d	260
			1.02 ^d	160
			0.055 ^e	110
$[\text{Cu}_2(\text{PTP})\text{Cl}_4]\cdot\text{CH}_3\text{CH}_2\text{OH}$ (III)	green	1.61	0.48 ^b	100
$[\text{Cu}_2(\text{PTP})_2](\text{I}_3)_2(\text{CH}_3\text{CN})_2$ (IV)	brown	diamag	0.60 ^d	110
			0.21	160
ferrocene ⁺⁰			0.37 ^b	85

^a Scan rate 200 mV s^{-1} . ^b Glassy carbon/ CH_3CN /TEAP. ^c Glassy carbon/DMF/TEAP. ^d Platinum/ CH_3CN /TEAP. ^e Glassy carbon/ Me_2SO /TEAP.

**Figure 5.** Magnetic susceptibility data for $[\text{Cu}_2(\text{PTP})\text{Cl}_4]\cdot\text{CH}_3\text{CH}_2\text{OH}$ (III). The solid line was calculated from eq 1 with $g = 2.029 \pm 0.004$, $-2J = 131 \pm 0.4 \text{ cm}^{-1}$, and $N\alpha = 60 \times 10^{-6} \text{ cgsu (cm}^3 \text{ mol}^{-1})/\text{Cu}$ and with the assumption of 0.38% paramagnetic impurity ($\rho = 0.0038$).

ordinated pyridine.²² The ligand PTP is characterized by a single, sharp pyridine absorption at 990 cm^{-1} . The binuclear copper(I) derivative II exhibits a strong perchlorate (ν_3) vibration at 1085 cm^{-1} , indicative of ionic perchlorate, and a single pyridine ring vibration at 1013 cm^{-1} , associated with coordinated pyridine. The crystal structure of $[\text{Cu}_2(\text{PTP})\text{Cl}_4]\cdot\text{CH}_3\text{CH}_2\text{OH}$ (III) has been reported,¹¹ and the binuclear cation consists of an asymmetrically bridged species involving a diazine and two chloro bridges (Figure 4). This species exhibits a single pyridine ring vibration in the infrared region at 1020 cm^{-1} , indicative of pyridine coordination, and a prominent visible absorption (mull transmittance) at 14900 cm^{-1} , typical of five-coordinate species of this sort. Compound IV, which contains the same binuclear copper(I) cation as II, has a basic infrared spectrum similar to that of II and an intense visible absorption at 22700 cm^{-1} , which is presumably associated with the triiodide anion.

The diamagnetic nature of II and IV corroborates the assignment of these compounds as copper(I) species, while compound I has a normal magnetic moment for a mononuclear copper(II) compound. The reduced room-temperature magnetic moment of compound III clearly indicates the presence of antiferromagnetic coupling between the copper(II) centers (Table VI). A variable-temperature magnetic study on III was carried out in the range 5–300 K. The results are summarized in Figure 5. The best-fit line was calculated from the Van Vleck equation²³ for exchange-coupled pairs of copper(II) ions (eq 1). In this expression

(16) Thompson, L. K.; Woon, T. C.; Murphy, D. B.; Gabe, E. J.; Lee, F. L.; LePage, Y. *Inorg. Chem.* **1985**, *24*, 4719.

(17) Bullock, G.; Harstock, F. W.; Thompson, L. K. *Can. J. Chem.* **1983**, *61*, 57.

(18) Mealli, C.; Arcus, C. S.; Wilkinson, J. L.; Marks, T. J.; Ibers, J. A. *J. Am. Chem. Soc.* **1976**, *98*, 711.

(19) Thompson, J. S.; Marks, T. J.; Ibers, J. A. *Proc. Natl. Acad. Sci. U.S.A.* **1977**, *74*, 3114.

(20) Nelson, S. M.; Trocha-Grimshaw, J.; Lavery, A.; McKillop, K. P.; Drew, M. G. B. *Biological and Inorganic Copper Chemistry*; Karlin, K. D., Zubieta, J., Eds.; Adenine: Gunderland, NY, 1985; p 27.

(21) Gabe, E. J.; Thompson, L. K., unpublished results.

(22) Thompson, L. K.; Chacko, V. T.; Elvidge, J. A.; Lever, A. B. P.; Parish, R. V. *Can. J. Chem.* **1969**, *47*, 4141.

(23) Van Vleck, J. H. *The Theory of Electric and Magnetic Susceptibilities*; Oxford University Press: London, 1932; Chapter 9.

$$\chi_m = \frac{N\beta^2 g^2}{3kT} [1 + \frac{1}{3} \exp(-2J/kT)]^{-1} (1 - \rho) + \left[\frac{N\beta^2 g^2}{4kT} \right] \rho + N\alpha \quad (1)$$

$2J$ (in the spin Hamiltonian $H = 2J\hat{s}_1 \cdot \hat{s}_2$) is the singlet-triplet splitting or exchange integral and other symbols have their usual meaning (ρ represents the fraction of a possible magnetically dilute copper(II) impurity). The temperature-independent paramagnetism for a binuclear copper(II) complex, $N\alpha$, was taken as 120×10^{-6} cgsu/mol, and the parameters giving the best fit were obtained by using a nonlinear regression analysis with ρ as a floating parameter. The exchange integral for III ($-2J$) was found to be 131 cm^{-1} , indicating modest spin exchange between the copper(II) centers.

The bridging network in III (Figure 4) involves an asymmetric arrangement of bridging chlorine atoms, with each chlorine bridge bonded via an axial and an equatorial interaction to the square-pyramidal copper atoms. This situation should effectively result in "no" spin exchange between the $d_{x^2-y^2}$ ground state copper(II) centers via the chlorine bridges. However, because the diazine bridge is bonded to both copper(II) centers via an equatorial interaction, this bridging pathway is considered to be responsible for the spin exchange. This situation contrasts with that observed for a series of hydroxide-bridged pyridylamino-phthalazine complexes, in which symmetric bridged structures involving two equatorial interactions to a hydroxide bridge led to much stronger spin exchange.^{9,22,24}

Compounds I and III are characterized by very positive reduction potentials. I displays nonreversible cyclic voltammograms with $E_{1/2} = +0.57 \text{ V}$ (vs. SCE) in acetonitrile (Table VI and ref 8), while III exhibits an almost reversible redox process at $E_{1/2} = +0.48 \text{ V}$ (vs. SCE) in acetonitrile with ΔE_p varying very slightly as a function of scan rate ($50\text{--}400 \text{ mV s}^{-1}$). The molar conductance of an acetonitrile solution of III is low ($\Lambda_M = 21 \Omega^{-1} \text{ cm}^2 \text{ mol}^{-1}$), indicating a largely undissociated species in this solvent. Controlled-potential electrolysis of III in acetonitrile at $+0.1 \text{ V}$ indicates the passage of 2 equiv of charge. During electrolysis the color of the solution gradually changes from green to colorless. Reoxidation of the reduced solution at $+0.70 \text{ V}$ restores the green color, and this solution has a visible absorption spectrum identical with that of the original solution. The triiodide derivative IV displays two distinct redox waves at $E_{1/2} = +0.21$ and $+0.60 \text{ V}$ in acetonitrile, which are associated with processes 2 and 3, respectively.^{25,26} The same voltammograms were obtained



by scanning in both positive and negative directions within the limits $+0.9$ and -0.2 V . Almost identical cyclic voltammograms can be generated from equimolar solutions of iodine and iodide in acetonitrile and from iodide alone in acetonitrile. This indicates that in this potential range the cycle voltammetry of IV is dominated by the triiodide ion. The binuclear perchlorate compound II, which contains the same cation as IV, displays rather unusual solvent-dependent cyclic voltammetry. In DMF a single, non-reversible wave is observed at $E_{1/2} = +0.19 \text{ V}$, while in Me_2SO a single, almost reversible, wave is observed at $E_{1/2} = +0.055 \text{ V}$. No other waves are observed in the range -0.3 to $+1.4 \text{ V}$ for both solvents. However, in acetonitrile, two distinct redox waves are observed in the same potential range at $E_{1/2} = +0.56$ and $+1.02 \text{ V}$, both of which appear to be nonreversible. The ligand PTP does not exhibit any electrochemical activity in this voltage range in these solvents. This high-potential wave can also be discerned as a weak feature in the cyclic voltammetry of IV when the scan

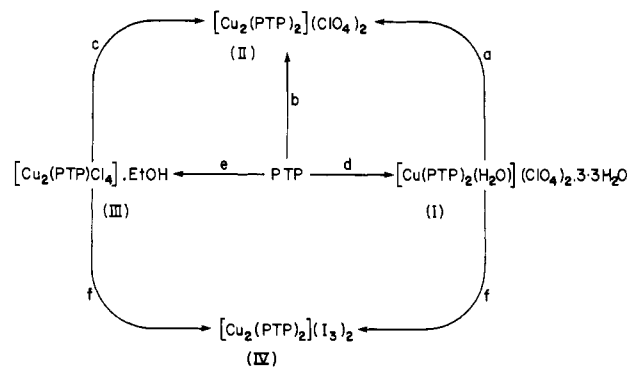


Figure 6. Synthetic scheme summarizing the coordination chemistry of PTP and the redox activity of I and III: (a) reflux in (1) MeOH or CH_3CN , (2) $\text{PPh}_3/\text{CH}_3\text{CN}$, or (3) $\text{SO}_3^{2-}/\text{H}_2\text{O}/\text{CH}_3\text{CN}$ or (4) coulometric reduction in CH_3CN ; (b) $[\text{Cu}(\text{CH}_3\text{CN})_4]\text{ClO}_4/\text{CH}_3\text{CN}$; (c) $\text{SO}_3^{2-}/\text{ClO}_4^-/\text{H}_2\text{O}$; (d) $\text{Cu}(\text{ClO}_4)_2 \cdot 6\text{H}_2\text{O}/\text{MeOH}$; (e) $\text{CuCl}_2 \cdot 2\text{H}_2\text{O}/\text{EtOH}$; (f) $\text{I}^-/\text{H}_2\text{O}$.

range is extended to $+1.5 \text{ V}$, but the wave at $+0.56 \text{ V}$ cannot be distinguished from the wave associated with the triiodide ion in this range. Controlled-potential electrolysis of a DMF solution of II at $+0.52 \text{ V}$ produced a green solution with passage of 2 equiv of charge, indicating a two-electron-oxidation process. In acetonitrile controlled-potential electrolysis of II at $+1.20 \text{ V}$ produce a green-blue solution with passage of 2 equiv of charge. Because of the broadness of the two waves in acetonitrile it was found impossible to separate the two steps coulometrically. However, peak height measurements suggest that each step involves a single electron transfer. The appearance of two waves for II in acetonitrile, with one at such a high potential, suggests that in this solvent the two metal centers are in different coordination environments. The wave at $+0.56 \text{ V}$ is at a substantially higher potential than the single waves observed in DMF and Me_2SO , indicating a stabilizing effect with respect to the copper(I) state in acetonitrile. This could be considered to be the result of solvent coordination to both copper centers in DMF and Me_2SO , which would lead to the stabilization of the copper(II) state. The two high-potential waves observed in acetonitrile could be the result of a situation where only one copper center is solvated. The high-potential wave ($+1.02 \text{ V}$) could then be associated with a copper center to which acetonitrile is bound (a stabilized copper(I) state), while the lower potential wave is associated with an unsolvated copper center. Conductance measurements indicate that compound II is a 1:2 electrolyte in both DMF and acetonitrile.

The redox activity of compounds I and III, which have markedly positive reduction potentials, can be exploited by reaction of these species with selective reducing agents that have reduction potentials in a suitable voltage range (Figure 6). Aqueous iodide will reduce both I and III with the formation of the binuclear copper(I) species IV. In both cases significant molecular rearrangement occurs in order to form what is obviously a very stable binuclear copper(I) cation. Aqueous and acetonitrile solutions of IV are stable, even on exposure to air. The analogous, stable copper(I) species II can be generated by reaction of PTP with cuprous perchlorate in acetonitrile (Experimental Section), reflux of I in methanol or acetonitrile, or by reaction of I with triphenylphosphine in acetonitrile or sulfite in aqueous acetonitrile (Figure 6). Also, coulometric reduction of I in CH_3CN produces II and the ligand PTP. III can also be converted to II by reaction with aqueous sulfite in the presence of excess perchlorate. However, on coulometric reduction in acetonitrile compound III appears to form a binuclear copper(I) species that does not rearrange to form the stable binuclear cation $[\text{Cu}_2(\text{PTP})_2]^{2+}$. This is supported by the ability of this compound to be reduced and oxidized coulometrically through several cycles with little apparent deterioration of the system and also the near-reversibility of the redox process at $+0.48 \text{ V}$.

Both the mononuclear derivative I and the binuclear derivative III have positive reduction potentials and produce the same binuclear copper(I) derivatives on reaction with sulfite and iodide.

(24) Thompson, L. K.; Hanson, A. W.; Ramaswamy, B. S. *Inorg. Chem.* **1984**, *23*, 2459.

(25) Popov, A. I.; Geske, D. H. *J. Am. Chem. Soc.* **1958**, *80*, 1340.

(26) Macagno, V. A.; Giordano, M. C.; Arvia, A. J. *Electrochim. Acta* **1969**, *14*, 335.

The binuclear copper(I) cation $[\text{Cu}_2(\text{PTP})_2]^{2+}$ represents an unusual, extremely stable copper(I) species, being unaffected in solution and in the solid state on exposure to air for extended periods of time. The formation of such a derivative from both binuclear and mononuclear copper(II) starting materials is remarkable, since it involves major molecular rearrangement, and emphasizes the significance of the redox activity of compounds of this sort. We are in the process of utilizing the unusual redox properties of this type of complex to effect intermolecular redox processes involving just copper(II) species. We have, for example, recently shown that compound III can selectively oxidize a binuclear copper(II) complex of a hexadentate phthalazine ligand, which has an oxidation potential ($E_{1/2} = +0.50$ V in DMF vs. SCE) in an appropriate range, to form a stable binuclear copper(III) derivative.²⁷

Acknowledgment. We thank the Natural Sciences and Engineering Research Council of Canada for financial support for this study, including the purchase of the variable-temperature Faraday susceptometer.

Registry No. I, 106856-02-4; II, 108712-00-1; III, 107424-54-4; $[\text{Cu}_2(\text{PTP})_2](\text{I}_3)_2$, 106855-97-4; $[\text{Cu}(\text{CH}_3\text{CN})_4]\text{ClO}_4$, 14057-91-1.

Supplementary Material Available: Tables SI and SIII, listing anisotropic thermal parameters for I and II, and Tables SV and SVI, listing bond length and angle data pertaining to the ligands in I and II (8 pages); Tables SII and SIV, listing observed and calculated structure factors for I and II (41 pages). Ordering information is given on any current masthead page.

(27) Mandal, S. K.; Thompson, L. K., unpublished results.

Contribution from the Chemical Crystallography Laboratory, Oxford University, Oxford OX1 3PD, England, and Brookhaven National Laboratory, Upton, Long Island, New York 11973

$\text{Ca}_{0.75}\text{Nb}_3\text{O}_6$: A Novel Metal Oxide Containing Niobium–Niobium Bonds. Characterization and Structure Refinement from Synchrotron Powder X-ray Data

S. J. Hibble,*^{1a} A. K. Cheetham,^{1a} and D. E. Cox^{1b}

Received December 24, 1986

A new mixed-metal oxide, $\text{Ca}_{0.75}\text{Nb}_3\text{O}_6$, has been characterized in the course of our investigations of the Ca–Nb–O system. The space group is *Immm* with cell constants $a = 7.113$ Å, $b = 10.286$ Å, and $c = 6.563$ Å. The structure was refined by using powder X-ray data obtained on the Brookhaven synchrotron. An extremely short Nb–Nb bond of 2.578 Å is present within an Nb_2O_8 unit.

Introduction

Many potentially interesting materials are found only as polycrystalline powders, and the lack of single crystals may preclude further study. In this paper we describe how analytical electron microscopy, combined with powder X-ray diffraction, can prove to be a powerful method for the characterization of polycrystalline materials. We further demonstrate that the high-resolution powder X-ray data obtainable from synchrotron radiation can allow the structural refinement of a novel compound present in a mixture. This methodology is especially appropriate to the investigation of complex phase diagrams of refractory oxides, as in the case considered here.

A large number of ternary oxides of molybdenum are known to contain metal clusters, for example $\text{Zn}_2\text{Mo}_3\text{O}_8$,² NaMo_4O_6 ,^{3a} $\text{Ba}_5(\text{Mo}_4\text{O}_6)_8$,^{3b} and $\text{La}_3\text{Mo}_4\text{SiO}_{14}$,⁴ but niobium, which is noted for its formation of octahedral Nb_6 clusters in its lower halides, appears to be less prone to metal–metal bonding in its oxide chemistry. The simple oxides NbO_5 and NbO_2 ⁶ do exhibit metal–metal bonding, but for the lower ternary oxides, cluster formation is only firmly established in the case of $\text{Mg}_3\text{Nb}_6\text{O}_{11}$.⁷

It would seem unlikely that the magnesium compound is unique, and we therefore attempted a systematic survey of the lower ternary oxides of niobium with the alkali and alkaline-earth metals.

We have investigated the ternary systems A–Nb–O with A = Ca, Sr, Ba, and K. A compound of composition $\text{Sr}_{\sim 0.7}\text{Nb}_4\text{O}_6$ ⁸ was prepared, which appears to be isomorphous with $\text{Ba}_5(\text{Mo}_4\text{O}_6)_8$ ³ and would therefore contain Nb clusters. We have also found isomorphous compounds containing Ba and K. In the Ca–Nb–O system, a new compound, $\text{Ca}_{0.75}\text{Nb}_3\text{O}_6$, was found and the lattice parameters indicated that this compound did not have a molybdenum analogue. The low average oxidation state for niobium made it probable that this compound contained Nb–Nb bonds. A structural investigation using a polycrystalline sample and a synchrotron X-ray source was therefore undertaken. After obtaining the synchrotron data, we learned of the then-unpublished work of Kohler and Simon⁹ on $\text{NaNb}_3\text{O}_5\text{F}$ and it appeared likely that this phase was isomorphous with ours. Their structural model, obtained from a single-crystal X-ray study, was used as the basis for our structural refinement.

Experimental Section

Synthesis and Analysis. A mixture of average stoichiometry CaNb_3O_6 was prepared from the appropriate mixture of CaCO_3 , Nb_2O_5 , and niobium metal. The carbonate was decomposed by reaction with Nb_2O_5 at 1400 °C, and the product was then ground with the appropriate amount of Nb metal and heated in vacuo in a sealed silica tube at 1250 °C. The product was a black powder.

A small quantity, ~25 mg, of the product was finely ground in an agate mortar and dispersed in ~2 mL of chloroform by an ultrasonic bath. A drop of this dispersion was placed on a 3-mm "Formvar"-coated copper grid and the solvent allowed to evaporate. X-ray microanalysis

- (1) (a) Oxford University. (b) Brookhaven National Laboratory. Work supported by the Division of Materials Science, U.S. Department of Energy, under Contract DE-AC02-76CH00016.
- (2) McCarroll, W. H.; Katz, L.; Ward, J. *J. Am. Chem. Soc.* **1957**, *79*, 5410.
- (3) (a) Torardi, C. C.; McCarley, R. E. *J. Am. Chem. Soc.* **1979**, *101*, 3963. (b) Torardi, C. C.; McCarley, R. E. *J. Less-Common Met.* **1986**, *116*, 169.
- (4) Betteridge, P. W.; Cheetham, A. K.; Howard, J. A. K.; Jakubicki, G.; McCarroll, W. H. *Inorg. Chem.* **1984**, *23*, 737.
- (5) Schafer, H.; Von Schneering, H. G. *Angew. Chem.* **1964**, *76*, 833.
- (6) Cheetham, A. K.; Rao, C. N. R. *Acta Crystallogr. Sect. B: Struct. Crystallogr. Cryst. Chem.* **1976**, *B32*, 1579.
- (7) Marinder, B.-O. *Chem. Scr.* **1977**, *11*, 97.

- (8) Hibble, S. J.; Cheetham, A. K. Presented at the Third European Conference on Solid State Chemistry, Regensburg, West Germany, 1986.
- (9) Kohler, J.; Simon, A. *Angew. Chem., Int. Ed. Engl.* **1986**, *25*, 996.